Biochemistry

pubs.acs.org/biochemistry

From the Bench

# Peptide-Dependent Growth in Yeast via Fine-Tuned Peptide/GPCR-Activated Essential Gene Expression

Sonja Billerbeck* and Virginia W. Cornish*

Cite This: *Biochemistry* 2022, 61, 150−159

Read Online

ACCESS | Metrics & More | Article Recommendations | Supporting Information

**ABSTRACT:** Building multicellular microbial consortia that communicate with each other and perform programmed functionalities is the next milestone for synthetic biology. Achieving cell−cell communication within these communities requires programming of the transduction of an extracellular signal into a customized intracellular response. G-protein-coupled receptors (GPCRs) are attractive candidates for engineering signal transduction as they can sense extracellular events with high sensitivity and specificity and transduce them into complex intracellular programs. We recently developed a scalable cell−cell communication language based on fungal mating GPCRs and their secreted peptide ligands. This language allows the assembly of engineered yeast strains into multicellular communication networks and allows them to be made interdependent by peptide signaling. In peptide signaling, one cell secretes a peptide that supports the growth of another cell at nanomolar concentrations, a scalable approach for engineering interdependence. Here we address the challenge of correlating the doubling time of *Saccharomyces cerevisiae* cells with an increasing external peptide concentration by linking GPCR activation to the expression of an essential gene. The required fine-tuning of downstream signaling is achieved via the transcriptional titration of a set of orthogonal GPCR-activated transcription factors, a series of corresponding promoters with different output dynamics, and the use of chemically recoded peptide ligands with varying activation potentials. As such, our work establishes three control points that allow the tuning of the basal and maximal activation of the GPCR response, fold change activation, and response sensitivity. The presented results enable the implementation of peptide-dependent and peptide-tunable growth but could also facilitate the design and calibration of more complex GPCR-controlled synthetic functionality in the future.

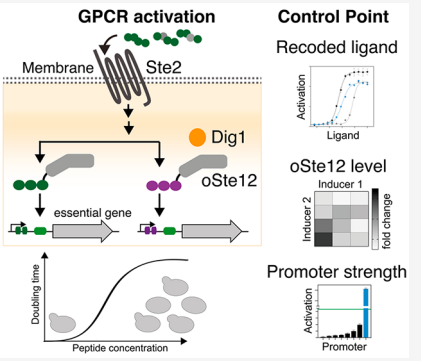


The capacity of cells to sense and respond to their environment and communicate with each other is a hallmark of biological behavior.[1,2] Extracellular molecular recognition followed by intracellular signal transduction has been widely leveraged for synthetic biology concepts, such as the engineering of biosensors[3−5] or the engineering of cell−cell communication in synthetic multicellular communities with applications in the emerging bioeconomy.[6−9] One prerequisite for harnessing cellular signaling pathways for synthetic functionalities is gaining precise control over their intracellular response architectures.

G-protein-coupled receptors (GPCRs) make up the largest group of eukaryotic membrane receptors, capable of recognizing virtually any signal from light to ions to small molecules and proteins with high sensitivity and specificity.[10] While the GPCR itself determines the molecular specificity of the extracellular sensing event, the cellular response depends on the underlying activated transcriptional program. The yeast *Saccharomyces cerevisiae* is a powerful synthetic biology host and has been shown to be a suitable chassis for the functional heterologous expression of several fungal GPCRs[7,11] and a subset of mammalian GPCRs, enabling cellular recognition of many different signals.[12] For instance, GPCRs in yeast have been harnessed for the detection of explosives,[13] as a screening tool for metabolic engineering,[14] and for basic studies of GPCR signaling.[12] Specifically for mammalian GPCRs, major past[15−17] and recent efforts[18−20] have been undertaken to enable functional coupling to the yeast mating pathway—although major improvements have been made, this is still a nontrivial challenge[12]—to facilitate the functional study of the various different classes of human GPCRs for basic science, biotechnology, and pharmacological applications. For example, currently only 6% of known human GPCRs have been demonstrated to functionally couple to the yeast pheromone pathway through chimeric engineering and only 11 of 17 total GPCR classes have any examples.[12]

We recently harnessed the group of fungal mating GPCRs to develop an array of low-cost yeast biosensors for pathogen detection,[4] and we repurposed these receptors and their peptide

**Received:** October 3, 2021
**Revised:** December 30, 2021
**Published:** January 13, 2022

ligands as interfaces in a scalable cell−cell communication language.[7]

This language allows the assembly of engineered yeast strains into multicellular communication networks and allows them to be made interdependent by peptide signaling. In peptide signaling, one cell secretes a peptide that supports the growth of another cell at nanomolar concentrations, a scalable approach for engineering interdependence.

One challenge is to precisely tune GPCR signaling, such that its dose-dependent output matches the functional expression levels of an essential gene.

This is required when engineering strains whose viability and doubling time are supposed to be controlled by the concentration of a GPCR-activating peptide input, secreted by another cell.

Here we engineer yeast strains that are stringently dependent on the presence of two different short peptide sequences and whose doubling times can be scaled with the peptide concentration in the nanomolar range, a concentration range that matches yeast peptide secretion levels.[7]

This is achieved by bringing the expression of the essential gene *SEC4* under the control of two different fungal mating GPCRs. By implementing three control points, two genetic control points and one chemical control point, we ensure that the GPCR dose−response curves match the expression level of our target essential gene. This guarantees low expression levels that do not allow for growth in the absence of a peptide and wild-type-like expression levels that support wild-type-like growth at peptide concentrations that induce full activation of the GPCR. Within the dynamic range of the GPCR, the peptide concentration determines the rate of growth of the engineered yeast cells.

While GPCR downstream signaling in yeast has been effectively re-engineered before[12]—for instance, the signal output has been optimized by model-guided tuning of the expression levels of the GPCR itself and its immediate downstream signaling proteins,[11] or the pathway output has been reshaped to be ultrasensitive, output-attenuated, or time-delayed by employing synthetic positive- and negative-feedback loops[21,22]—all of these studies have implemented biosensor-type sense-report systems that require the activation of the reporter gene with a quick and strong signal and a large dynamic range.

Here we implement viability and input-dependent doubling times as GPCR-controlled functions. We show that very fine-tuned GPCR signaling in the low-expression regime is essential for achieving this engineering goal, a requirement that is different from previously implemented strong reporter readouts.

To achieve the correct GPCR tuning, we required several engineering rounds and the availability of our modular control points proved to be essential for effective troubleshooting.

## RESULTS AND DISCUSSION

**Engineering Goal and Approach.** Our engineering goal was to create a set of *S. cerevisiae* strains that are stringently dependent on the presence of a GPCR-activating peptide ligand (no growth in the absence of the peptide ligand) and, further, whose doubling time can be controlled in a peptide concentration-dependent manner in the low nanomolar range. We have shown before that GPCR-peptide ligands can be secreted by yeast in nanomolar concentrations. As such, sensors and secretors can be interconnected into synthetic yeast communities by peptide signaling.[7]

To achieve our goal, we developed a framework consisting of three control points that in total allow for very tight control over peptide/GPCR-induced gene expression. In addition, we aimed to create a framework that, once established, could be scaled to more complex gene expression programs beyond controlling a single gene.

Two of the three control points involve genetic reconstruction of the yeast strains, while the third control point involves chemical changes within the peptide ligand. First, we used the expression level of orthogonal variants (oSte12s) of the central transcriptional regulator Ste12 to tune basal activation, maximal activation, and the on/off fold change of a readout. Second, we used a promoter library to further tune the basal expression of the readout gene. Third, we used the amino acid code of the peptide ligand to tune the sensitivity ($EC_{50}$) of GPCR activation. To make the system insulated and scalable, we designed orthogonal Ste12 transcription factor/promoter pairs based on exchangeable synthetic zinc finger DNA-binding domains (ZF-DBDs). ZF-DBDs recognize unique 9 bp operator sites in a synthetic promoter without cross-talk, and a large toolbox of orthogonal domains that can be multiplexed is available to the synthetic biology community (Figure 1 and Supplementary Figure 1).[23,24] As such, they allow for true scalability of the oSte12 activation profile, when compared to the limited set of natural DNA-binding domains that have been used in previous engineered Ste12 designs.[11]

Eventually, we envision that several of these oSte12s can be co-expressed in a cell, each regulating its own set of genes, as such enabling the complexity of a given GPCR-activated genetic program to be scaled (Supplementary Figure 1).

**System Design.** The central transcription factor Ste12 activates downstream gene expression in the natural *S. cerevisiae* mating response after the mating GPCRs Ste2 and Ste3 have been activated by their corresponding mating pheromones α- and a-factor, respectively [α-factor is a 13-residue unmodified peptide, WHWLQLKPGQPMY (Supplementary Figure 1)].[25] In the absence of a pheromone, Ste12 is regulated by the proteins Dig1 and Dig2. Dig1 and Dig2 inhibit the transcriptional activation role of Ste12; additionally, Dig2 stabilizes the Ste12 protein, leading to a large pool of inactive Ste12 in a non-pheromone-induced cell.[25,26] Pheromone treatment causes the Ste12/Dig1/Dig2 complex to dissociate, due to MAP-kinase-mediated phosphorylation of all three proteins, leading to derepression of Ste12 and consequently the activation of downstream gene expression.[27] As such, Ste12 inhibition is based on reversible stoichiometric protein−protein interactions. Here we harnessed the concept that the stoichiometric ratio between the transcriptional activator Ste12 and its repressor proteins Dig1 and Dig2 can be harnessed to control basal gene expression (leakiness) and the fold change in expression from a single promoter.[11] We then tested if the concept holds for several engineered orthogonal Ste12 variants (oSte12s) that decouple GPCR activation from the natural mating response by using zinc finger-based DNA-binding domains that feature different DNA activation domains when wired to user-defined synthetic promoters (Supplementary Figure 1 outlines their design). Next, using the expression level of the oSte12 variants (in relation to Dig1) as a first set point, we designed a set of modular oSte12-responsive promoters (OSRps) that allow further titration of gene expression levels to reach the required "tightness" (no leaky expression) and activatability (fold change activation) to achieve peptide-controllable growth when used in combination with an essential gene. We used a set of available


https://doi.org/10.1021/acs.biochem.1c00661
Biochemistry 2022, 61, 150−159

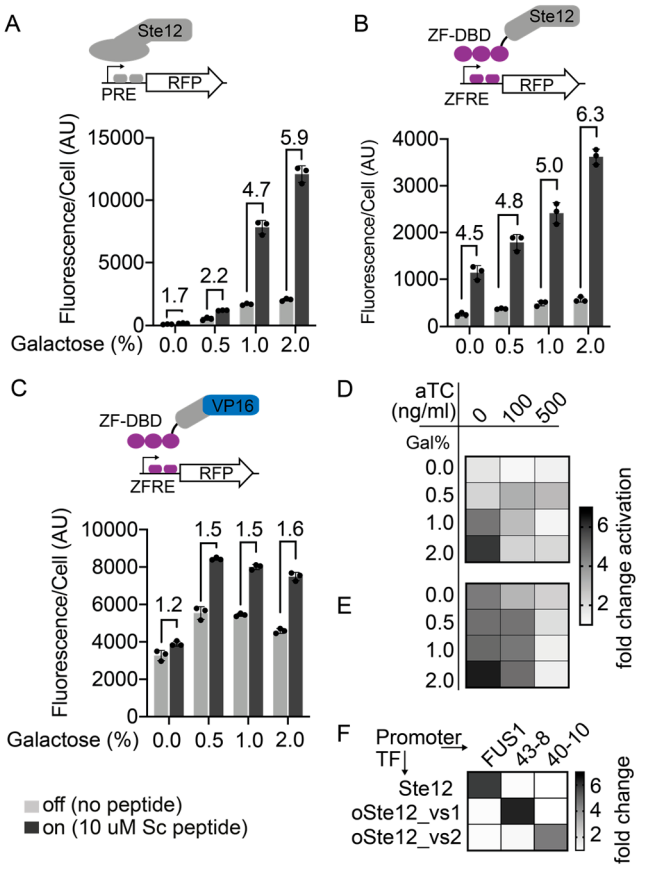


**Figure 1.** Activation profile of wild-type Ste12 and oSte12s with increasing expression levels. Strain ySB02 was transformed with plasmids pSB11, pSB13, and pSB14 with plasmid pSB47 or pSB14 (Supplementary Table 3) encoding oSte12_vs1.1, oSte12_vs1.2, and Ste12, respectively, and the oSte12_vs1.1-responsive promoter 8xZFRE43-8-CYC 1p or the FUS 1p driving a yEmRFP as readout, respectively. Cells were cultured in 96-well format in the presence of the indicated concentration of galactose and/or aTC and in the presence or absence of 10 $\mu$M Sc peptide. Fluorescence was measured after cells had grown for 20 h. (A) Activation profile of oSte12_vs1.1 with increasing galactose concentrations. Note that the galactose and aTC inducible promoter GalTetO that was used in this study shows leaky expression even in the absence of aTC. This is why we included 0 ng/mL aTc as an induction value. The numbers indicate the fold change difference between the induced and uninduced state. (B) Activation profile of Ste12. (C) Activation profile of oSte12_vs1.2. (D and E) Fold change activation profile for Ste12 and oSte12_vs1.1, respectively, across all tested induction conditions. (F) Fold change activation at increasing aTC and galactose concentrations. The highest fold change in activation was reached at 100 ng/mL aTc and 2% galactose. Error bars in panels A−C represent the standard deviation (SD) of three measurements using three individual transformants for each construct.

synthetic minimal yeast promoters as core promoters,[28] which eventually yielded short synthetic pheromone inducible promoters (~200−300 bp) that are completely orthogonal to the yeast genome.

As the third control point, we harnessed the fact that the exact amino acid sequence of the mating GPCR-activating peptide ligands determines their activation potential ($EC_{50}$).[7] As such, recoded peptide ligands, with single amino acids exchanged, could be used to shift the sensitivity to further fine-tune it. In the following, we describe the systematic testing of each control point.

**Control Point 1: Transcriptional Titration of the Engineered Orthogonal Ste12 Variants Allows the Tuning of Basal Activation, Maximal Activation, and the On/Off Fold Change of a Readout.** To explore if the expression ratio between our engineered orthogonal Ste12 variants and Dig1/Dig2 can be harnessed for tuning transcriptional activation, we placed the natural Ste12 and its orthogonal derivatives oSte12_vs1.1 and oSte12_vs1.2 (Supplementary Figure 1) under control of a previously described TetR-controlled GAL1 promoter.[24] This allowed us to titrate the Ste12 and oSte12 expression levels with increasing concentrations of galactose and anhydrotetracycline (aTc) while keeping the expression level of Dig1 and Dig2 constant (chromosomally encoded, endogenous expression level). As a readout, we used a plasmid-encoded red fluorescent protein (yEmRFP) either under control of the FUS1 promoter (for activation of the natural Ste12) or under the control of a CYC1 promoter featuring eight repetitive zinc finger-responsive elements (ZFREs) for oSte12_vs1.1 and oSte12_vs1.2 activation (Supplementary Figure 3 and Supplementary Table 3).[24] We constructed an *ste12* deletion strain with the chromosomal copy of *ste12* replaced with a methionine selection marker [ySB02 (Supplementary Table 1)] as a test chassis. The endogenous Sc.Ste2 mating GPCR expressed by ySB02 served as a test GPCR, and synthetic $\alpha$-factor (Sc peptide) was used as the ligand for activation. We grew cells in the presence of combinatorically increasing amounts of aTC and galactose, with or without 10 $\mu$M Sc peptide treatment, and we recorded fluorescence after growth for 24 h. Panels A−C of Figure 1 show that increasing expression levels of Ste12, oSte12_vs1.1, and oSte12_vs1.2 lead to increased levels of basal activation but also allowed for an overall increased level of pathway activation after the addition of the Sc peptide. For all constructs, there was an optimal induction combination that allowed for the highest level of fold change activation (Figure 1D,E). Very high expression levels lead to full activation even in the absence of a peptide. Likely, Dig1 and Dig2 concentrations became restrictive in repressing the high levels of available Ste12 and oSte12. In addition, it was shown that Ste12 degradation follows saturating kinetics, leading to a longer half-life of Ste12 in mutants expressing higher levels of Ste12.[26]

In summary, these results indicated that, in a range, changing the expression level of the oSte12s while keeping Dig1 and Dig2 expression levels constant could be used to set the basal activation of the pathway, the overall response intensity, and the fold change in activation, as long as Ste12 was not strongly expressed leading to constitutive pathway activation.

In addition, the identity of the transcriptional activation domain within our engineered oSte12s determined pathway activation and fold change; oSte12_vs1.1 features the natural Ste12 activation domain, while oSte12_vs1.2 uses the strong virus-derived VP16 activation domain (Supplementary Figure 1). The strong VP16 activation domain in oSte12_vs1.2 showed higher levels of basal activation even at low oSte12 expression levels and lower levels of fold change activation after the addition of the peptide when compared to those of the Ste12-derived activation domain in oSte12_vs1.1 (Figure 1B,C). Overall, the natural Ste12 activation domain gave better control over peptide-induced gene activation, and as such, oSte12_vs1.1 was used for the remainder of the study.

**The Number of Orthogonal Transcription Factors Can Be Scaled by the Replacement of the Zinc Finger-Binding Domain (ZF-DBD).** Orthogonal Ste12 transcription


https://doi.org/10.1021/acs.biochem.1c00661
Biochemistry 2022, 61, 150−159

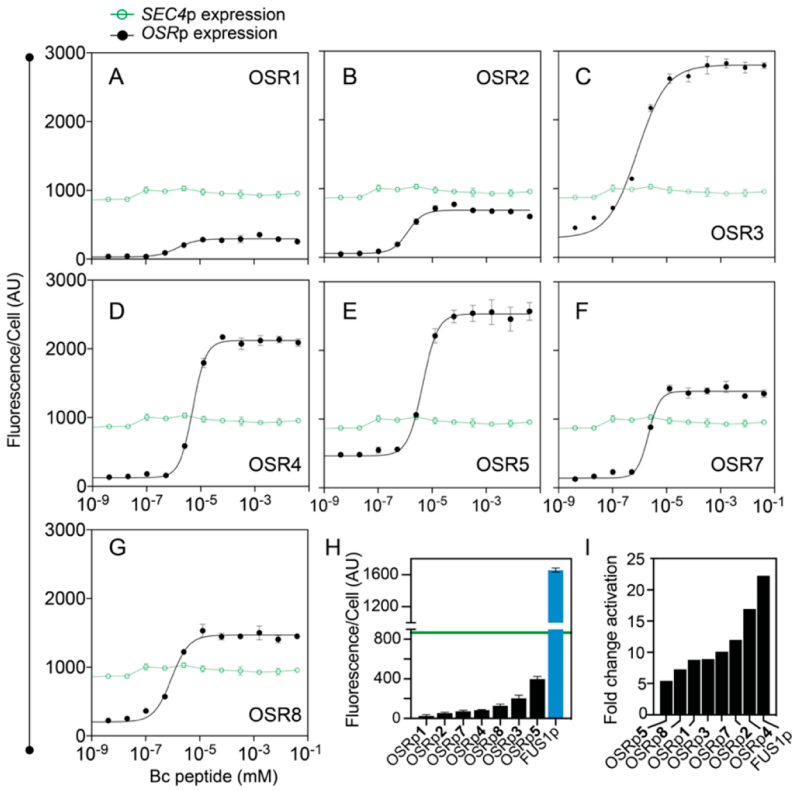


**Figure 2.** Dose−response curves of *OSR*ps in comparison to expected Sec4 expression levels. Strain ySB138 (Bc.Ste2) was transformed with all *OSR*p readout plasmids (Supplementary Tables 2 and 3). Cells were cultured in 96-well format and induced with 5-fold dilutions of the synthetic Bc peptide (starting with 40 $\mu$M). Fluorescence was measured after growth for 8 h. The green line displays the fluorescence derived from the expression level of the SEC4 promoter across peptide concentrations: (A) OSR1 (pSB49), (B) OSR2 (pSB48), (C) OSR3 (pSB66), (D) OSR4 (pSB67), (E) OSR5 (pSB68), (F) OSR7 (pSB70), and (G) OSR8 (pSB49). (H) Basal expression from the OSRps in the absence of the Bc peptide (compared to FUS 1p in blue, plasmid pSB14). (I) Fold activation of the OSR promoters (average maximal activation divided by average basal activation), organized by increasing number. Error bars in panels A−H represent the standard deviation of three measurements using three individual transformants for each construct.

factors have been engineered previously by employing bacterial or yeast DNA-binding domains such as those from the LexA or the Gal4 transcription factors.[14,29] We chose to build our oSte12s by using zinc finger DNA-binding domains (ZF-DBDs). ZF-DBDs can be customized to bind user-defined 9 bp operator sequences[23,30] and have been used to build synthetic (non-inducible) transcription factors previously.[24] As such, they constituted an ideal resource for building an extendable set of oSte12s by simply exchanging the DNA-binding domain. To test this, we replaced the 43-8 ZF-DBD[23] in oSte12_vs1.1 with the ZF-DBD 42-10,[23] and we exchanged the operator sites in the promoter (Supplementary Figure 1). The resulting transcription factor oSte12_vs2.1 showed a similar activation profile with increasing aTC and galactose concentrations (Supplementary Figure 2). In addition, Ste12, oSte12_vs1.1, and oSte12_vs2.1 were indeed orthogonal to each other and did not induce expression from the other promoters (Figure 1F). As such, they can be used together to activate downstream gene expression with different activation profiles set by their expression level.

**Control Point 2: A Set of Short Synthetic Promoters Further Fine-Tune Basal Activation and Fold Change, Which Are Critical to Achieving Peptide-Dependent Growth in a GPCR-Specific Manner.** As a second control point, we designed a set of orthogonal Ste12-responsive promoters (OSRps) that could be activated by our oSte12s. The specific design constraint for this study was to generate very tight promoters that showed no or very little expression in the absence of a peptide but could match the natural expression levels of a target essential gene to be brought under GPCR control to engineer peptide-dependent strains. Herein, we chose to use the essential gene *SEC4* because of its favorable performance in previous gene-essentiality studies that made it likely suitable for our design.[31,32] First, the gene product of *SEC4*, a Ras-related GTPase required for exo- and endocytosis, is essential under all growth conditions (unconditionally essential), and *SEC4* can thus be used to implement strains that stringently depend solely on the presence of a peptide ligand for viability. Second, when *SEC4* was placed under an inducible promoter in a previous study,[32] strains showed robust growth in the presence of the inducer but complete failure to grow in the absence of the inducer. In agreement with the robust growth under *SEC4*-inducing conditions, the proteome and transcriptome of these strains were almost unchanged under these conditions,[32] indicating that yeast cells can tolerate variations in the *SEC4* expression levels (e.g., robustly tolerate higher than endogenous levels) while losing viability when expression levels fall under a certain threshold, which was an important feature for implementing our peptide-signaling design. Noteworthy, at this point we did not yet know whether *SEC4* levels could become growth rate determining, meaning that certain expression levels could be used to control the doubling time. Other genes that showed similar features and could be useful to explore for future


https://doi.org/10.1021/acs.biochem.1c00661
Biochemistry 2022, 61, 150−159

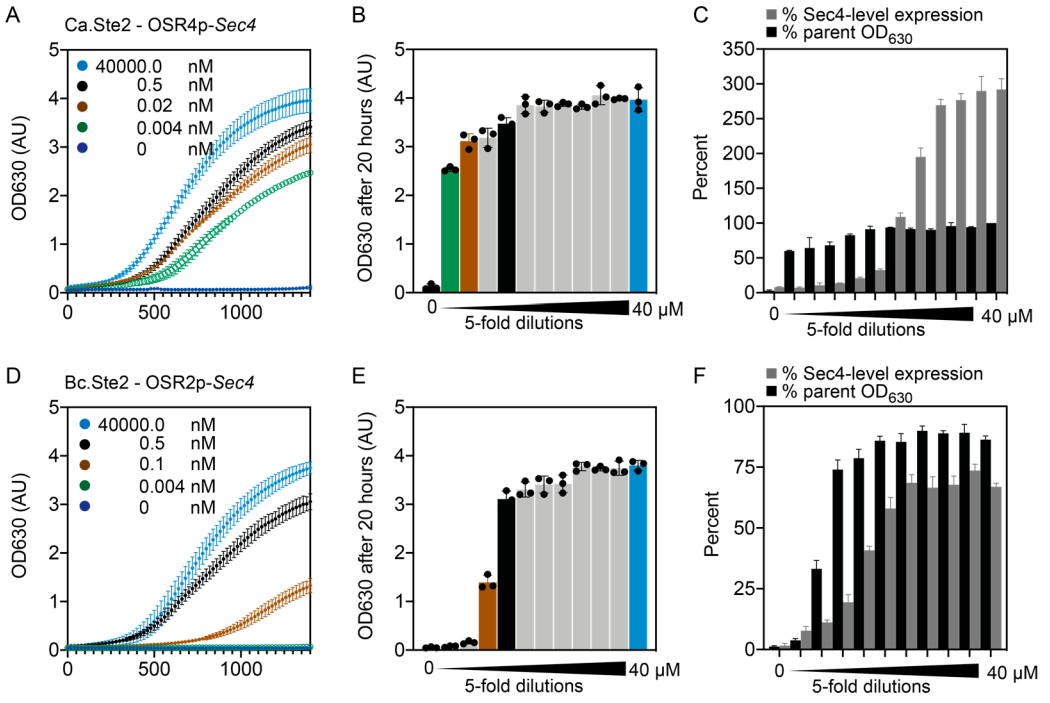


**Figure 3.** Peptide concentration-dependent growth. Yeast strains ySB265 (*OSR2*p-SEC4, Bc.Ste2) and ySB267 (*OSR4*p-SEC4, Ca.Ste2) were cultured for 20 h in the presence or absence of the indicated concentrations of peptide (see the text and Supplementary Figure 6 for preculturing conditions). The optical density (OD) of the culture (absorbance at 630 nm) was recorded every 20 min. (A) Growth of ySB267 over time upon incubation with growth-determining concentrations of Ca peptide. (B) Final OD of ySB267 across all tested Ca peptide concentrations. Colored bars correspond to the colors in panel A. (C) Comparison between the final $OD_{630}$ of ySB267 (presented as the percentage of the final $OD_{630}$ of parent strain ySB139) and the fluorescence derived from the OSR4 promoter assay [presented as the percentage of the *SEC4* promoter assay (Figure 2)]. (D) Growth of ySB265 over time upon incubation with growth-determining concentrations of Bc peptide. (E) Final OD of ySB265 across all tested Bc peptide concentrations. (F) Comparison between the final $OD_{630}$ of ySB264 (presented as the percentage of the final $OD_{630}$ of parent strain ySB138) and the fluorescence derived from the OSR2a promoter assay [presented as the percentage of the *SEC4* promoter assay (Figure 2)]. Error bars in panels A, B, D, and E represent the standard deviation of three measurements using three individual single-colony isolates of strains ySB265 and ySB267. Error bars in panels C and F represent the standard deviation of three measurements using three individual transformants (gray bars, data derived from plasmid-based fluorescence assay) or single-colony isolates of strains ySB265 and ySB267 (black bars, growth assay).

peptide-signaling designs are *FAS2* and *RBP11*.[32] For promoter construction, we developed a modular assembly strategy using a set of natural and synthetic minimal core promoters,[28] varying repeats of an upstream repressing sequence (URS),[33] and varying repeats of a zinc finger response element (ZFRE), here using the ZFRE corresponding to ZF 43-8.[23] In total, we constructed seven different OSR promoters (Supplementary Figure 3 and Supplementary Table 3). To be able to compare *SEC4* expression levels with the expression levels of the designed OSR promoters (OSRps), we linked the *SEC4* promoter and the OSRps to red fluorescent protein (yEmRFP) expression. We then constructed a strain with fixed expression levels of oSte12_vs1.1 by replacing the natural *STE12* gene with the gene encoding oSte12_vs1.1 using our previously engineered peptide/GPCR language strain as a parent.[7] To test the system with different mating GPCRs, we replaced the endogenous Sc.Ste2 with the orthogonal GPCRs Bc.Ste2 and Ca.Ste2; both had previously shown a high level of orthogonality and very high sensitivity ($EC_{50}$ in the low nanomolar range) for their peptide ligand.[7]

The new strains were designated ySB138 (featuring oSte12_vs1.1 and Bc.Ste2) and ySB139 (featuring oSte12_vs1.1 and Ca.Ste2). Both strains were transformed with all seven OSRp reporter plasmids as well as with the *SEC4*p reporter plasmid. Dose−response curves were measured using increasing concentrations of synthetic Bc or Ca peptides. Figure 2 shows that the promoters featured small increments of basal activation [approximately 3−40% of the expected *SEC4* expression level (Figure 2H)], maximal activation (approximately 27−267%), and different degrees of fold change [5−17-fold (Figure 2I)]. Similar results were obtained upon activation of the same promoters via Ca.Ste2 in strain ySB139 (Supplementary Figure 4). Most importantly, several promoters showed very low basal expression levels (in the absence of a peptide) but still reached the expression level of *SEC4* when induced. For instance, OSR2 in combination with Bc.Ste2 allowed expression from 5% of the *SEC4* level to 63% under full induction, OSR7 from 7% to 142%, and OSR4 from 9% to 223%. Interestingly, the natural *FUS1* promoter in combination with both Bc.ste2 and Ca.Ste2 showed already basal activation levels (177%) in the absence of a peptide that were higher than the expected expression levels of the *SEC4* promoter; as such, the FUS1 promoter could not have been used for essential strain engineering (Figure 2H and Supplementary Figure 4H).

**Controlling Growth via GPCR Signaling.** Next, we combined the first two control points to implement yeast strains that were stringently dependent on peptide and whose growth rate could be controlled by increasing concentrations of a peptide ligand in the nanomolar range. While we measured the expected strength of the *SEC4* promoter in comparison to those of our OSR promoters, it remained a matter of testing at which expression levels the Sec4 protein concentrations would


https://doi.org/10.1021/acs.biochem.1c00661
Biochemistry 2022, 61, 150−159

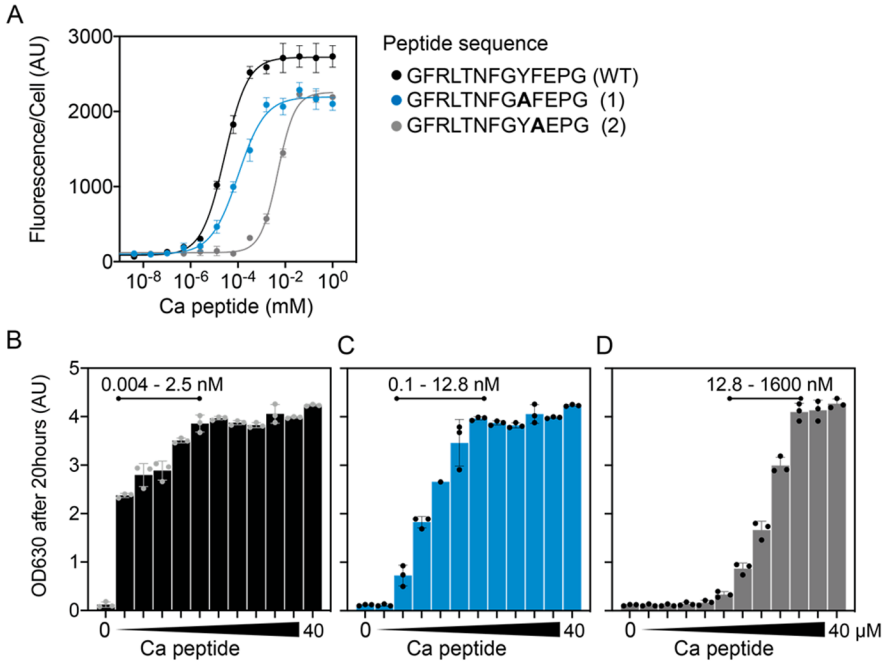


**Figure 4.** Growth can be modulated by single-residue exchanges in the peptide ligand. (A) Dose−response curve for strain ySB139 (Ca.Ste) transformed with pSB66 (*OSR4*p). Cells were cultured in 96-well format and induced with 5-fold dilutions of synthetic Ca peptide (starting with 100 $\mu$M) or its recoded peptide derivatives. Fluorescence was measured after growth for 8 h. (B−D) Final $OD_{630}$ values of ySB267 when cultured with decreasing concentrations of Ca peptide (5-fold dilutions of synthetic Ca peptide, starting with 40 $\mu$M) and its derivatives 1 (C) and 2 (D). The concentration range that allowed for the tuning of growth is indicated for each peptide (actually tested peptide concentrations are given). Error bars in panel A represent the standard deviation of three measurements using three individual transformants. Error bars in panels B−D represent the standard deviation of three measurements using three individual single-colony isolates of strain ySB267.

decrease below the levels required for cellular viability (no growth) and at what range the Sec4 levels would become growth-determining (tunable growth rate). We, therefore, tested three promoters (OSR1, -3, and -4) that showed different basal activation levels lower than the *sec4* expression levels [OSR1 > OSR4 > OSR3 (Figure 2H)] but also different maximal activation levels lower than (OSR2) or higher than the Sec4 levels (OSR3 and OSR4). We used CRISPR/Cas9 to insert the OSRps right upstream of the Sec4 gene. Strains ySB138 and ySB139 were used as parents, and cells were grown in the presence of 500 nM Bc or Ca peptide during the CRISPR procedure to maintain *SEC4* expression after homology-based promoter replacement. While we could successfully recover *SEC4* promoter replacements for OSR3 and OSR4 for both strains (ySB138 and ySB139), we could recover only OSR2 replacements in ySB138. This promoter potentially shows too little expression when combined with Ca.Ste2 to yield viable strains. In addition, after locus sequencing, we observed deletion of three of the eight repetitive ZF elements for the OSR2 promoter. However, when cloned and tested with a red fluorescence protein as a readout, the ZFRE deletion did not significantly impact the dose−response curve of OSR2 (Supplementary Figure 5). Still, the results of the CRISPR procedure indicate that the protocol needs to be optimized to work flawlessly with the repetitive sequences used herein.

We chose four strains for further growth analysis: ySB138 and ySB139 with OSR3p-*SEC4*, ySB138 with OSR2*ap*-*SEC4*, and ySB139-OSR4ap-*SEC4* [ySB284, ySB284, ySB265, and ySB267, respectively (Supplementary Table 1)].

First, we tested the number of doublings required to achieve peptide dependence after peptide removal. Strains were routinely maintained on media supplemented with 500 nM peptide (GPCR-activated). As such, we expected that achieving peptide dependence would require several doublings to "dilute" excess Sec4 protein and silence its expression. Peptide-dependent growth was therefore measured over several growth/dilution cycles (Supplementary Figure 6). Interestingly, for the OSR3p-driven *SEC4* strains, peptide dependence could not be reached and the strains grew like their parent strains even in the absence of peptide (Supplementary Figure 6A,C), indicating the basal activation of OSR3 was already enough to provide enough Sec4 protein for growth. For the OSR2-driven and OSR4-driven *SEC4* strains ySB265 and ySB267, we observed the expected behavior of peptide dependence (Figure 3 and Supplementary Figure 6B,D). After approximately six or seven doublings, strains stopped growing in the absence of peptide and maintained a rate of growth comparable to (ySB267) or >80% (ySB265) of that of their parent in the presence of 500 nM peptide (full induction) (Supplementary Figure 7). We then tested growth of ySB265 and ySB267 at increasing peptide concentrations (Figure 3). The rate of growth of ySB265 could be controlled by Bc peptide between 0.1 and 0.5 nM. The strain did not grow at the tested concentrations of <0.1 nM and reached its maximum growth rate at the tested concentrations of >0.5 nM (Figure 3D,E and Supplementary Figure 8). For ySB267, growth could be controlled by Ca peptide between 0.004 and 2.5 nM and reached its maximum growth rate at the tested concentrations of >2.5 nM (Figure 3A,B and Supplementary Figure 9). We correlated the *SEC4* and OSR promoter assay data (derived from Figure 2 and Supplementary Figure 5, a proxy for the expected expression levels of *SEC4*) with these growth data. For both strains, more


https://doi.org/10.1021/acs.biochem.1c00661
*Biochemistry* 2022, 61, 150−159

than 50−60% of *SEC4* levels were needed to re-establish >85% growth (measured as the final OD) (Figure 3C,F).

**Control Point 3: Recoding of the Peptide Ligand Allows the Scaling of the Sensitivity Window of Peptide Concentration-Dependent Growth.** Being able to shift the growth sensitivity of a strain to its peptide ligand could facilitate the implementation of interdependent yeast consortia as it would give flexibility in matching the secretion level of a given peptide sequence to the desired growth rate of a strain within a community. We have previously shown that single-residue changes in the peptide ligand can lead to changes in the corresponding GPCR's response characteristics. Strain ySB267 showed a dynamic growth-controllable range that spanned 3 orders of magnitude in the picomolar to low nanomolar range. We were interested if this window could be shifted by using recoded peptide ligands with different activation potentials.

We chose two recoded Ca peptides that we had previously identified via alanine scanning[7] and confirmed their shift in $EC_{50}$ with our herein developed oSte12 setup (Figure 4A). Ca peptide-1 showed an approximately 4-fold higher $EC_{50}$ and peptide-2 an approximately 177-fold higher $EC_{50}$ compared to that of the wild-type Ca peptide (Supplementary Table 4). Most importantly, growth in the presence of increasing concentrations of these recoded ligands allowed a shift in the dynamic range of the GPCR response (Figure 4B−D). Peptide-1 allowed for the dynamic control of the growth rate over 2 orders of magnitude in the low nanomolar range, specifically from 0.1 to 12.8 nM (actually measured concentrations). Peptide-2 allowed for the dynamic control of growth over 2 orders of magnitude in the midnanomolar to low micromolar range, specifically from 12.8 and 1630 nM. Taken together with the dynamic range achieved by the original Ca peptide (low picomolar to low nanomolar range, 0.004 and 2.5 nM), our ligand recoding approach allows a user to tune the growth rate of a strain in a ligand concentration window of 6 orders of magnitude without the need for genetic re-engineering of the actual strain by simply choosing a suitable recoded ligand.

## CONCLUSION

Here we present a three-step experimental framework for tuning GPCR downstream signaling that enabled the engineering of yeast strains that are stringently dependent on a peptide input and whose doubling times scale with the peptide concentration.

We learned that implementing GPCR-controlled growth needed very fine-tuned gene expression to be effective. When expression levels were off balance, cells were not viable at all or they grew even in the absence of peptide. As such, the availability of a set of modular control points proved to be essential for effective troubleshooting and navigating through various rounds of engineering.

We first showed that the expression level and the identity of the activation domain of our orthogonal Ste12 derivatives (oSte12s) can be harnessed to set the basal activation, maximal activation, and fold change of a readout gene. Once the basal oSte12 expression was fixed, we used a set of synthetic oSte12-responsive promoters (OSR promoters) to identify oSte12/promoter pairs that showed dose−response curves that meander around the expression level of our target essential gene *SEC4* (no activation in the absence and full expression levels in the presence of peptide). The three most promising pairs were then used to implement yeast strains that are stringently dependent on the presence of a peptide ligand and whose doubling time can be controlled in a concentration-dependent manner. One of the three tested promoters (OSR3) showed overly high basal activity and impaired the achievement of peptide dependence. A second promoter (OSR2) yielded peptide-dependent strains with tunable growth but could not re-establish full growth rates at full induction. The third promoter (OSR4) was suitable for engineering the anticipated dependence on peptide and the anticipated control over doubling time, highlighting the impact that subtle differences in GPCR output can have toward reaching an engineering goal. Finally, we established that the peptide concentration range that allows for growth rate control can be shifted by using recoded peptide ligands. For example, here we achieve a shift in the peptide/GPCR $EC_{50}$ values [measured by fluorescence (Figure 4a and Supplementary Table 4)] from 27 nM to 101 and 4800 nM by single-residue recoding. Recoded peptide ligands that activate fungal mating GPCRs with the desired activation potential can thereby be identified by simple alanine scanning of the original ligand, which is a feasible approach, as affordable chemically synthesized peptide ligands are commercially available.

While the use of recoded peptides is specifically suited for peptide-activated GPCRs such as the herein used fungal mating GPCRs or the human peptide-responsive GPCRs that have been shown to functionally couple to the yeast mating pathway,[12] the two other presented control points should be readily suitable for tuning responses of other classes of GPCRs that have been functionally expressed in yeast.[12] The many ongoing efforts to engineer functional expression of more classes of human GPCRs in yeast[18−20] indicate that many more GPCR/ligand pairs will be available in the future.

In addition, the herein engineered small synthetic pheromone inducible promoters that are orthogonal to the yeast genome, in combination with our first control point (the oSte12 expression levels), are designed to be scalable in number. Upon exchange of the zinc finger DNA-binding domain of the oSte12 transcription factor for one of the many available orthogonal zinc finger versions,[23] many oSte12 variants can likely be multiplexed and used to control orthogonal synthetic pheromone inducible promoters. As such, more complex genetic programs beyond the control of a single gene could be envisioned. The feasibility of achieving complex GPCR-mediated genetic programs is exemplified by the natural mating response itself. Mating GPCR signaling leads to the activation of a 200-gene program that induces complex phenotypic changes eventually driving the cell into cell cycle arrest and sexual reproduction.[25] On the molecular level, this includes large transcriptional changes for some genes but subtle changes for others.[34]

While our work addresses the issue of GPCR activation in the low-output regime as well as it allows for scalability, combining our control points with existing resources such as model-guided MAP-kinase pathway tuning to achieve high-level output[4,11] and resources that allow for temporal modulation of downstream signaling[21,22] should facilitate the design and calibration of more complex GPCR-controlled synthetic programs.

In summary, the presented results enable the implementation of peptide-dependent and peptide-tunable growth that is required for the assembly of interdependent consortia of yeast, where differently engineered cells support each other's growth via secretion of peptide ligands. Distributing synthetic biology tasks across multiple strains is a powerful approach for overcoming the current engineering limit of single strains.[9,35]

In addition, our strains could be a useful resource for IP protection (IP-protected engineered strains can be propagated


https://doi.org/10.1021/acs.biochem.1c00661
Biochemistry 2022, 61, 150−159

only in the presence of an undisclosed ingredient) and biocontainment.[36,37]

## METHODS

**Materials.** Synthetic peptides (≥95% purity) were obtained from GenScript (Piscataway, NJ). *S. cerevisiae* α-factor was obtained from Zymo Research (Irvine, CA). Polymerases, restriction enzymes, and Gibson assembly mix were obtained from New England Biolabs (NEB, Ipswich, MA). Components of media were obtained from BD Bioscience (Franklin Lakes, NJ) and Sigma-Aldrich (St. Louis, MO). Primers and synthetic DNA (gBlocks) were obtained from Integrated DNA Technologies (IDT, Coralville, IA). Plasmids were cloned and amplified in *Escherichia coli* C3040 (NEB). Sterile, black, clear-bottom 96-well microtiter plates and transparent round-bottom microtiter plates were obtained from Corning (Corning Inc.). Anhydrotetracycline was obtained from Sigma-Aldrich.

**Media.** Synthetic dropout medium (SD) was supplemented with appropriate amino acids and 2% glucose; fully supplemented medium containing all amino acids with uracil and adenine is termed synthetic complete (SC). For induction with galactose, SD medium was supplemented with 2% raffinose instead of 2% glucose and supplemented with the indicated concentrations of galactose (final concentration of 0.5%, 1%, or 2%). Yeast strains were also cultured in YEPD medium. *E. coli* was grown in Luria Broth (LB) medium. To select for *E. coli* plasmids with drug-resistant genes, ampicillin (Sigma-Aldrich) was used at a final concentration of 200 μg/mL. Agar was added to a final concentrations of 2% to prepare solid yeast media.

**CRISPR/Cas9 System.** The herein used Cas9 and guide RNA (gRNA) expression plasmids were used as described previously[7] (Supplementary Tables 5 and 6). For engineering yeast using the Cas9 system, cells were first transformed with the Cas9-expressing plasmid. Following a co-transformation of the gRNA-carrying plasmid and a repair fragment, single colonies were then verified using colony PCR primers binding upstream and downstream of the locus, and the resulting PCR product was then subjected to Sanger sequencing. Primers are listed in Supplementary Table 7.

**Yeast Strains.** All *S. cerevisiae* strains used in this study are listed in Supplementary Table 1, and those introduced in this study were constructed as follows.

*Construction of ySB02.* ySB02 is a derivative of BY4733 with *STE12* replaced by a *METH15* cassette. The strain was used for transcriptional titration of the orthogonal oSte12s. ySB02 was constructed by replacing *STE12* with a *METH15* expression cassette using homologous recombination followed by selection for methionine auxotrophic colonies. Primers SB372−SB378 (Supplementary Table 7) were used to amplify the *METH15* selection cassette and to add homology arms for recombination with the Ste12 locus. pRS411 was used as a template.

*Construction of Strains ySB138 and ySB139.* ySB138 and ySB139 are derivatives of yNA899 and were used to characterize the OSR promoters as well as the modulator peptides. The strains were constructed in two steps using the CRISPR/Cas9 system described above and the gRNAs and repair fragments listed in Supplementary Table 6. First, we chromosomally integrated oSte12_vs1.1 by replacing the DNA-binding domain of wild-type Ste12 (residues 1−215) with zinc finger-based DNA-binding domain 43-8. This resulted in oSte12_vs1.1 being under the control of the natural *STE12* promoter. The corresponding strain was called ySB137. ySB137 was then used to integrate the expression cassettes for Bc.Ste2 and Ca.Ste2 into the Δ*STE2* locus as described previously.[7] The resulting strains were called ySB138 (Bc.Ste2) and ySB139 (Ca.Ste2).

*Construction of Yeast Strains ySB265, ySB267, ySB284, and ySB285.* These strains were used to assay the dependence of growth on the peptide. ySB138 and ySB139 were used as the parents, and construction was achieved by using the CRISPR/Cas9 system described above and the gRNAs and repair fragments listed in Supplementary Table 4. We replaced the natural *SEC4* promoter in ySB138 with OSR2p (ySB265; note that this strain eventually encodes OSR2ap) and OSR3p (ySB284) as well as in ySB139 with OSR4p (ySB265) and OSR3p (ySB285). Cells were grown in the presence of 500 nM peptide during the CRISPR/Cas9 engineering to maintain cellular viability.

**Plasmids.** All plasmids used in this study are listed in Supplementary Table 5.

**Transcriptional Titration Assay.** Titration of Ste12 and the oSte12s from the TetR-controlled GAL1 promoter was performed in yeast strain ySB02. ySB02 was transformed combinatorially with two plasmids: first with the plasmid encoding the Ste12 or oSte12 variant [pSB11, pSB13, pSB27, or pSB252, each a pRS414 derivative (Supplementary Table 5)], and second with the plasmid encoding the fluorescent readout [pSB47 or pSB14, each a pRS413 derivative (Supplementary Table 3)]. Three individual transformants were picked and used as biological replicates to allow triplicate measurements for Figure 1A−C. The three transformants were individually cultured overnight in SC medium containing 2% raffinose without the selective components tryptophan and histidine. The next day, transformants were seeded into SD medium containing 2% raffinose and increasing concentrations of galactose (0.5%, 1%, and 2%). Each galactose concentration was additionally supplemented with increasing amounts of aTc (0, 100, and 500 ng/mL). Yeast strains were assayed in 96-well microtiter plates using a total volume of 200 μL and cultured at 30 °C and 800 rpm. Cells were seeded at an $OD_{630}$ of 0.3 (all herein reported cell density values are based on $OD_{630}$ measurements in 96-well plates with a volume of 200 μL for cultures with a path length of ∼0.3 cm performed in a SynergyMx plate reader from BioTek). Red fluorescence (excitation at 588 nm, emission at 620 nm) and culture turbidity ($OD_{630}$) were measured after 12 h. Because the optical density values were outside the linear range of the photodetector, all optical density values were first corrected using the following formula to give true optical density values:

$$OD_{true} = \frac{k \times OD_{meas}}{OD_{sat} - OD_{meas}} \quad (1)$$

where $OD_{meas}$ is the measured optical density, $OD_{sat}$ is the saturation value of the photodetector, and $k$ is the true optical density at which the detector reaches half-saturation of the measured optical density. All fluorescence values were then normalized by the true $OD_{630}$.

**GPCR Dose−Response Assays.** The response in fluorescence readout to increasing doses of a synthetic peptide ligand was measured in strain ySB138 or ySB139 transformed with one of the OSRp plasmids under investigation [plasmids pSB47−pSB49 and pSB66−pSB70 (Supplementary Table 5)]. Three individual transformants were picked for each promoter and used as biological replicates to allow triplicate measurements for Figure 2A−H, Figure 4A, Supplementary Figure 4A−


https://doi.org/10.1021/acs.biochem.1c00661
Biochemistry 2022, 61, 150−159

H, and Supplementary Figure 5. The three transformants for each construct were assayed in 96-well microtiter plates using a total volume of 200 $\mu$L and cultured at 30 °C and 800 rpm. Cells were seeded at an $OD_{630}$ of approximately 0.3 in SC medium without histidine (selective component). Red fluorescence (excitation at 588 nm, emission at 620 nm) and culture turbidity ($OD_{630}$) was measured after 8 h using a SynergyMx plate reader (BioTek), and the optical density was corrected as described above. Dose responses were measured at different concentrations (11 5-fold dilutions in $H_2O$ starting at 40 $\mu$M peptide; $H_2O$ was used as the no peptide control; for data in Figure 4A, 11 5-fold dilutions starting at 100 $\mu$M peptide were measured) of the appropriate synthetic peptide ligand. All fluorescence values were normalized by the true $OD_{630}$ and plotted against the log(10)-converted peptide concentrations. Data were fit to a four-parameter nonlinear regression model using Prism (GraphPad).

**Growth Assays.** The growth of strains under investigation was measured in 96-well plates using a total culture volume of 200 $\mu$L, and the cells were cultured at 30 °C in the SynergyMx plate reader (high rate of orbital shaking). To perform triplicate measurements, the CRISPR-engineered and sequence-verified strains ySB265, ySB267, ySB284, and ySB285 were streaked on agar plates to isolate single colonies. Three colonies were picked and used as replicates in Figure 3 and Supplementary Figures 7−9. The three isolates for each strain were individually cultured overnight. The next day, cells were seeded at an $OD_{630}$ of approximately 0.08 in SC medium and culture turbidity ($OD_{630}$) was recorded every 20 min for 20 h. Growth rates were extracted from the linear range of the $Y = \ln(Y)$-converted graphs using linear regression. In the case of peptide-dependent growth, cells were cultured in the presence of different peptide concentrations (11 5-fold dilutions in $H_2O$ starting at 40 $\mu$M peptide; $H_2O$ was used as the no peptide control). After growing for 20 h, cell cultures were normalized to the true $OD_{630}$ of 4 and diluted 1:50 in fresh medium.

## ■ ASSOCIATED CONTENT

### Supporting Information

The Supporting Information is available free of charge at https://pubs.acs.org/doi/10.1021/acs.biochem.1c00661.

Supplementary Figures 1−9 and Tables 1−7 (PDF)

### Accession Codes

ScSte2 (*S. cerevisiae*), D6VTK4; BcSte2 (*Botrytis cinerea*), G2YE05_BOTF4; CaSte2 (*Candida albicans*), A0A1D8PTB4; Ste12 (*S. cerevisiae*), P13574.

## ■ AUTHOR INFORMATION


### Corresponding Authors

**Virginia W. Cornish** − *Department of Chemistry, Columbia University, New York, New York 10027, United States;* Email: vc114@columbia.edu

**Sonja Billerbeck** − *Molecular Microbiology, Groningen Biomolecular Sciences and Biotechnology Institute, University of Groningen, 9700 AB Groningen, The Netherlands; Department of Chemistry, Columbia University, New York, New York 10027, United States;* orcid.org/0000-0002-3092-578X; Email: s.k.billerbeck@rug.nl

Complete contact information is available at: https://pubs.acs.org/10.1021/acs.biochem.1c00661



### Funding

This research was funded by DARPA Grant HR0011-15-2-0032.

### Notes

The authors declare no competing financial interest.


## ■ ACKNOWLEDGMENTS


The authors thank Neta Agmon and Jef Boeke (New York University Langone Health) for helpful discussions, especially on how to use the URS element, and for kindly providing strain yNA899 and we thank Mo Khalil (Boston University) for proving plasmids pL111, pL115, and pL278.


## ■ REFERENCES


(1) Szathmáry, E.; Smith, J. M. The major evolutionary transitions. *Nature* **1995**, *374*, 227−232.

(2) Rokas, A. The origins of multicellularity and the early history of the genetic toolkit for animal development. *Annual Review of Genetics* **2008**, *42*, 235−251.

(3) Rider, T. H.; et al. A B cell-based sensor for rapid identification of pathogens. *Science (80-.).* **2003**, *301*, 213−215.

(4) Ostrov, N.; Jimenez, M.; Billerbeck, S.; Brisbois, J.; Matragrano, J.; Ager, A.; Cornish, V. W. A modular yeast biosensor for low-cost point-of-care pathogen detection. *Sci. Adv.* **2017**, *3*, e1603221.

(5) Hicks, M.; Bachmann, T. T.; Wang, B. Synthetic Biology Enables Programmable Cell-Based Biosensors. *ChemPhysChem* **2020**, *21*, 132−144.

(6) Morsut, L.; et al. Engineering Customized Cell Sensing and Response Behaviors Using Synthetic Notch Receptors. *Cell* **2016**, *164*, 780−791.

(7) Billerbeck, S.; Brisbois, J.; Agmon, N.; Jimenez, M.; Temple, J.; Shen, M.; Boeke, J. D.; Cornish, V. W. A scalable peptide-GPCR language for engineering multicellular communication. *Nat. Commun.* **2018**, *9*, 5057.

(8) Du, P.; Zhao, H.; Zhang, H.; Wang, R.; Huang, J.; Tian, Y.; Luo, X.; Luo, X.; Wang, M.; Xiang, Y.; Qian, L.; Chen, Y.; Tao, Y.; Lou, C. De novo design of an intercellular signaling toolbox for multi-channel cell−cell communication and biological computation. *Nat. Commun.* **2020**, *11*, 4226.

(9) Qian, X.; Chen, L.; Sui, Y.; Chen, C.; Zhang, W.; Zhou, J.; Dong, W.; Jiang, M.; Xin, F.; Ochsenreither, K. Biotechnological potential and applications of microbial consortia. *Biotechnol. Adv.* **2020**, *40*, 107500.

(10) Schiöth, H. B.; Lagerström, M. C. Structural diversity of g proteincoupled receptors and significance for drug discovery. *Nat. Rev. Drug Discovery* **2008**, *7*, 339−357.

(11) Shaw, W. M.; et al. Engineering a Model Cell for Rational Tuning of GPCR Signaling. *Cell* **2019**, *177*, 782−796.e27.

(12) Lengger, B.; Jensen, M. K. Engineering G protein-coupled receptor signalling in yeast for biotechnological and medical purposes. *FEMS Yeast Res.* **2020**, *20*, 87.

(13) Radhika, V.; et al. Chemical sensing of DNT by engineered olfactory yeast strain. *Nat. Chem. Biol.* **2007**, *3*, 325−330.

(14) Mukherjee, K.; Bhattacharyya, S.; Peralta-Yahya, P. GPCR-Based Chemical Biosensors for Medium-Chain Fatty Acids. *ACS Synth. Biol.* **2015**, *4*, 1261−1269.

(15) King, K.; Dohlman, H. G.; Thorner, J.; Caron, M. G.; Lefkowitz, R. J. Control of yeast mating signal transduction by a mammalian beta 2-adrenergic receptor and Gs alpha subunit. *Science* **1990**, *250*, 121−123.

(16) Price, L. A.; Kajkowski, E. M.; Hadcock, J. R.; Ozenberger, B. A.; Pausch, M. H. Functional coupling of a mammalian somatostatin receptor to the yeast pheromone response pathway. *Mol. Cell. Biol.* **1995**, *15*, 6188−6195.

(17) Brown, A. J.; Dyos, S. L.; Whiteway, M. S.; White, J. H. M.; Watson, M.-A. E. A.; Marzioch, M.; Clare, J. J.; Cousens, D. J.; Paddon, C.; Plumpton, C.; Romanos, M. A.; Dowell, S. J. Functional coupling of mammalian receptors to the yeast mating pathway using novel yeast/mammalian G-protein $\alpha$-subunit chimeras. *Yeast* **2000**, *16*, 11−22.

(18) Rowe, J. B.; Taghon, G. J.; Kapolka, N. J.; Morgan, W. M.; Isom, D. G. CRISPR-addressable yeast strains with applications in human G protein-coupled receptor profiling and synthetic biology. *J. Biol. Chem.* **2020**, *295*, 8262−8271.
(19) Kapolka, N. J.; et al. Dcyfir: A high-throughput CRISPR platform for multiplexed G protein-coupled receptor profiling and ligand discovery. *Proc. Natl. Acad. Sci. U. S. A.* **2020**, *117*, 13117−13126.
(20) Bean, B. D. M. Functional expression of opioid receptors and other human GPCRs in yeast engineered to produce human sterols. *bioRxiv* **2021**, DOI: 10.1101/2021.05.12.443385.
(21) Bashor, C. J.; Helman, N. C.; Yan, S.; Lim, W. A. Using engineered scaffold interactions to reshape MAP kinase pathway signaling dynamics. *Science (80-.)* **2008**, *319*, 1539−1543.
(22) Ng, A. H.; et al. Modular and tunable biological feedback control using a de novo protein switch. *Nat. 2019 5727768* **2019**, *572*, 265−269.
(23) Maeder, M. L.; et al. Rapid 'Open-Source' Engineering of Customized Zinc-Finger Nucleases for Highly Efficient Gene Modification. *Mol. Cell* **2008**, *31*, 294−301.
(24) Khalil, A. S.; et al. A synthetic biology framework for programming eukaryotic transcription functions. *Cell* **2012**, *150*, 647−658.
(25) Bardwell, L. A walk-through of the yeast mating pheromone response pathway. *Peptides* **2005**, *26*, 339−350.
(26) Houser, J. R.; Ford, E.; Nagiec, M. J.; Errede, B.; Elston, T. C. Positive roles for negative regulators in the mating response of yeast. *Mol. Syst. Biol.* **2012**, *8*, 586.
(27) Olson, K. A.; et al. Two Regulators of Ste12p Inhibit Pheromone-Responsive Transcription by Separate Mechanisms. *Mol. Cell. Biol.* **2000**, *20*, 4199−4209.
(28) Redden, H.; Alper, H. S. The development and characterization of synthetic minimal yeast promoters. *Nat. Commun.* **2015**, *6*, 7810.
(29) Pi, H.; Chien, C. T.; Fields, S. Transcriptional activation upon pheromone stimulation mediated by a small domain of Saccharomyces cerevisiae Ste12p. *Mol. Cell. Biol.* **1997**, *17*, 6410−6418.
(30) Beerli, R. R.; Barbas, C. F. Engineering polydactyl zinc-finger transcription factors. *Nat. Biotechnol.* **2002**, *20*, 135−141.
(31) Mnaimneh, S.; et al. Exploration of essential gene functions via titratable promoter alleles. *Cell* **2004**, *118*, 31−44.
(32) Agmon, N.; et al. Low escape-rate genome safeguards with minimal molecular perturbation of Saccharomyces cerevisiae. *Proc. Natl. Acad. Sci. U. S. A.* **2017**, *114*, E1470−E1479.
(33) Vidal, M.; Brachmann, R. K.; Fattaey, A.; Harlow, E.; Boeke, J. D. Reverse two-hybrid and one-hybrid systems to detect dissociation of protein-protein and DNA-protein interactions. *Proc. Natl. Acad. Sci. U. S. A.* **1996**, *93*, 10315−10320.
(34) MacKay, V. L.; et al. Gene expression analyzed by high-resolution state array analysis and quantitative proteomics. *Mol. Cell. Proteomics* **2004**, *3*, 478−489.
(35) Zhou, K.; Qiao, K.; Edgar, S.; Stephanopoulos, G. Distributing a metabolic pathway among a microbial consortium enhances production of natural products. *Nat. Biotechnol.* **2015**, *33*, 377−383.
(36) Torres, L.; Krüger, A.; Csibra, E.; Gianni, E.; Pinheiro, V. B. Synthetic biology approaches to biological containment: Pre-emptively tackling potential risks. *Essays Biochem.* **2016**, *60*, 393−410.
(37) Lee, J. W.; Chan, C. T. Y.; Slomovic, S.; Collins, J. J. Next-generation biocontainment systems for engineered organisms. *Nat. Chem. Biol.* **2018**, *14*, 530−537.


https://doi.org/10.1021/acs.biochem.1c00661
*Biochemistry* 2022, 61, 150−159